Sensors and Actuators B 182 (2013) 424–428

Contents lists available at SciVerse ScienceDirect

Sensors and Actuators B: Chemical

journal homepage: www.elsevier.com/locate/snb

Sensitivity enhanced biosensor using graphene-based one-dimensional photonic crystal

Kandammathe Valiyaveedu Sreekanth[a], Shuwen Zeng[b,c], Ken-Tye Yong[b], Ting Yu[a,d,*]

[a] Division of Physics and Applied Physics, School of Physical and Mathematical Sciences, Nanyang Technological University, 21 Nanyang Link, Singapore 637371, Singapore
[b] School of Electrical and Electronic Engineering, Nanyang Technological University, Singapore 639798, Singapore
[c] CINTRA CNRS/NTU/THALES, UMI 3288, Research Techno Plaza, 50 Nanyang Drive, Border X Block, Singapore 637553, Singapore
[d] Department of Physics, Faculty of Science, National University of Singapore, 3 Science Drive, Singapore 117542, Singapore

ARTICLE INFO

Article history:
Received 22 October 2012
Received in revised form 16 February 2013
Accepted 13 March 2013
Available online 22 March 2013

Keywords:
Graphene
Surface electromagnetic waves
Surface plasmon
Photonic crystal

ABSTRACT

In this paper, we propose and analytically demonstrate a biosensor configuration based on the excitation of surface electromagnetic waves in a graphene-based one-dimensional photonic crystal (1D PC). The proposed graphene-based 1D photonic crystal consists of alternating layers of high (graphene) and low (PMMA) refractive index materials, which gives a narrow angular reflectivity resonance and high surface fields due to low loss in PC. A differential phase-sensitive method has been used to calculate the sensitivity of the configuration. Our results show that the sensitivity of the proposed configuration is 14.8 times higher compared to those of conventional surface plasmon resonance (SPR) biosensors using gold thin films. This novel and effective graphene-based 1D PC will serve as a promising replacement of metallic thin film as a sensor head for future biosensing applications.

1. Introduction

In the past decade, surface plasmon (SP) concept has found tremendous applications in variety of areas such as biosensors, solar cells, lithography, etc. [1–4]. The SP based biosensors for instance has enabled high speed and high sensitive biomolecular detection. This is mainly because they eliminate time-consuming labeling process and reduce molecular binding disturbance compared to commonly employed fluorescence based optical biosensors. However, the damping of light intensity caused by the metal absorption loss affects the sensitivity of biosensors for various applications [5,6]. In this context, excitation of surface electromagnetic waves (SEWs) in one-dimensional (1D) photonic crystals (PC) has been investigated for various potential applications such as sensors, fluorescence emission enhancement, and enhancement of the Goos–Hänchen effect [7–10]. Surface electromagnetic waves are non-radiative electromagnetic modes that appear on the surface of semi-infinite 1D photonic crystal, which is considered to be an alternative to surface plasmon [11,12]. The low loss in photonic crystals may provide higher intensity of SEWs, which leads to much sharper resonance dips and high surface electromagnetic fields. More recently, our group has been experimentally demonstrated the excitation of surface electromagnetic waves in a graphene-based 1D PC using prism coupling technique [13].

Since graphene is a single two-dimensional plane of carbon atoms forming a hexagonal lattice, the optical properties of graphene has been extensively investigated both theoretically and experimentally for many photonics and optoelectronics applications due to its strong interaction with light in a broad wavelength interval [14–17]. In particular, graphene exhibits universal optical conductivity from visible to infrared frequencies due to interband transition [18]. Recently, graphene-based photonic crystals at THz frequencies have been proposed and theoretically investigated for the development of frequency filters and waveguides [19]. The photonic crystal waveguide analogy of graphene nanoribbons have been theoretically investigated by Benisty [20]. More recently, Yan, et al. has reported the fabrication of tunable infrared plasmonic devices using photonic crystal like structure (graphene/insulator stacks) [21]. These reported works may provide an effective way in designing graphene-based optoelectronics devices. In addition, graphene has been recently started using in surface plasmon resonance biosensor to enhance the adsorption of biomolecules and hence to improve the sensitivity of the biosensors [22–25]. Here, we propose a biosensor configuration based on the excitation of surface electromagnetic waves in a graphene-based 1D photonic crystal and analytically investigate the sensitivity of the configuration.

* Corresponding author at: Division of Physics and Applied Physics, School of Physical and Mathematical Sciences, Nanyang Technological University, 21 Nanyang Link, Singapore 637371, Singapore. Tel.: +65 6316 7899; fax: +65 6316 6984.
E-mail address: yuting@ntu.edu.sg (T. Yu).

0925-4005/$ – see front matter
http://dx.doi.org/10.1016/j.snb.2013.03.039

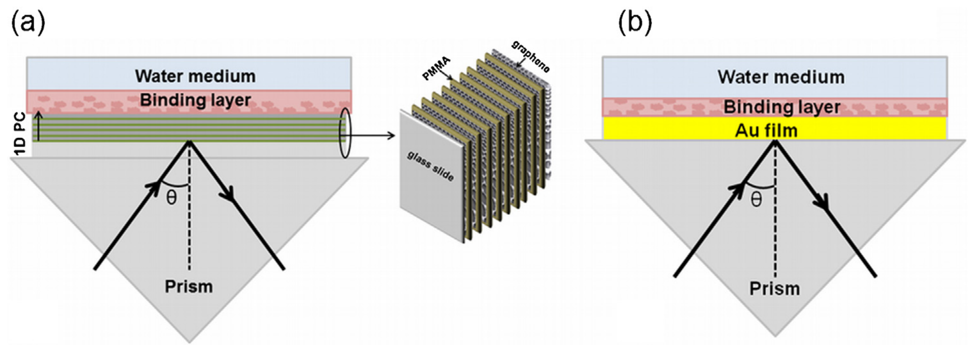

Fig. 1. Schematic diagram of (a) proposed biosensor configuration and (b) surface plasmon resonance biosensor. Graphene-based 1D photonic crystal consists of alternating layers of graphene and PMMA layers with an additional graphene termination layer.

2. Theory

The schematic diagram of proposed biosensor configuration based on prism coupling technique is shown in Fig. 1(a). The graphene-based 1D PC is attached via index matching fluid on the top of the BK7 glass prism. The binding layer of thickness 3 nm and refractive index 1.462 (n_3) is assumed as a ssDNA layer with a density of 0.028 g/cm^2,which is prepared in water and covers the whole PC [23]. The graphene-based 1D PC consists of alternating layers of high and low refractive index materials such as graphene and poly methyl methacrylate (PMMA), respectively deposited on the BK7 glass slide. The wavelength of excitation light source is taken as 633 nm. Here, we assume that the graphene is a dielectric material with isotropic refractive index and light polarization does not affect on graphene refractive index because of the universal opacity of graphene at optical frequencies. The refractive index of graphene calculated at 633 nm wavelength is $n_1 = 3 + 1.149\,i$ [26]. The refractive index of BK7 prism (n_0), PMMA (n_2) and water (n_4) is taken as 1.515, 1.49 and 1.33, respectively. The thicknesses of graphene and PMMA are taken as $0.34 \times L$ nm (d_1) (where $L = 1$, number of graphene layer) and 470 nm (d_2), respectively. The proposed periodic structure represents a Bragg grating with a Bragg wavelength of 1.4 μm (calculated using $\lambda_B = 2(n_1 d_1 + n_2 d_2)$). The designed 1D PC consists of complete 9 bilayers of graphene/PMMA with an additional graphene termination layer. It is possible to move the surface mode dispersion through the photonic bands from one edge to the other when the termination layer of the photonic crystal is varied [27]. In order to compare the results of proposed configuration, conventional surface plasmon resonance biosensor geometry is also investigated (as shown in Fig. 1(b)). In Fig. 1(b), the metal is taken as Au film with thickness 45 nm. The refractive index of Au at 633 nm wavelengths is $0.1968 + 3.09\,i$ [28]. The remaining parameters are same as those of proposed configuration (Fig. 1(a)).

In order to determine the sensitivity of both configurations, a differential phase sensitive method has been employed [29,30]. In this method, a standard Mach–Zehnder interferometer setup can be used to extract the phase difference between the interfering signal of TM-polarization (signal) and TE-polarization (reference). The phase difference between TM- and TE-polarization is given by, $\Delta\phi = \phi_{TM} - \phi_{TE}$. The values of ϕ_{TM} and ϕ_{TE} can be extracted from the Fresnel's reflection coefficients of TM- and TE-polarization, $r_{TM} = |r_{TM}| \exp(i\phi_{TM})$ and $r_{TE} = |r_{TE}| \exp(i\phi_{TE})$, respectively. The reflectance ($(r^2_{TM,TE} = R)$) of TM- and TE-polarization can be calculated by solving the Fresnel's equations for N-layer model using transfer matrix method (TMM). Here, the reflectance (R) is a serial product of the interface matrix I_{jk} ($j = 0, 1, 2, 3$ and $k = j + 1$), and layer matrix L_j [31].

$$R = \left| \frac{M_{12}}{M_{22}} \right|^2 \quad (1)$$

with

$$M = \begin{bmatrix} M_{11} & M_{12} \\ M_{21} & M_{22} \end{bmatrix},\ I_{jk} = \begin{bmatrix} 1 & r_{jk} \\ r_{jk} & 1 \end{bmatrix} \ \text{and}\ L_j = \begin{bmatrix} e^{ik_{zj}d_j} & 0 \\ 0 & e^{-ik_{zj}d_j} \end{bmatrix} \quad (2)$$

where d_j is the thickness of jth layer, and

$$k_{zj} = \sqrt{\varepsilon_j \left(\frac{2\pi}{\lambda}\right)^2 - k_x^2} \quad (3)$$

In the case of TM polarization

$$r_{jk} = \frac{((k_{zj}/\varepsilon_j) - (k_{zk}/\varepsilon_k))}{((k_{zj}/\varepsilon_j) + (k_{zk}/\varepsilon_k))} \quad (4)$$

In the case of TE polarization

$$r_{jk} = \frac{((k_{zj}/\sqrt{\varepsilon_j \varepsilon_k}) - (k_{zk}/\sqrt{\varepsilon_j}\varepsilon_k))}{((k_{zj}/\sqrt{\varepsilon_j \varepsilon_k}) + (k_{zk}/\sqrt{\varepsilon_j}\varepsilon_k))} \quad (5)$$

In Eq. (3), k_x is the parallel wave vector, and given by $k_x = n_0(2\pi/\lambda)\sin\theta$, where λ is excitation wavelength and θ is the incident angle.

3. Results and discussion

Based on the TMM method, the reflectance data is simulated separately for both configurations. The excitation of surface electromagnetic wave is recognized as the angle at which minimum reflected intensity is occurred (ATR minimum) and this ATR minimum angle is taken as the resonance angle. Fig. 2(a) represents the reflectance diagram of proposed configuration using TM-polarization. From the figure, it is evident that the obtained resonance angle is 79.2°, which is greater than the angle for total internal reflection (TIR) between prism and water (61.3°). Hence this deepest dip at resonance angle corresponds to the non-radiative SEW propagating at the 1D PC/binding layer boundary. Fig. 2(b) shows the reflectance curve obtained for surface plasmon resonance biosensor and observed resonance angle is 75.25°. It is visible from the Fig. 2 that the proposed biosensor configuration provides a deepest, narrow dip as compared to surface plasmon resonance biosensor. It shows that the graphene-based 1D PC has low loss and maximum surface mode excitation compared to surface plasmon resonance biosensor.

The sensitivity of the biosensor is defined as, $S = (\Delta\phi/\Delta n_3)E$, where the first term ($\Delta\phi/\Delta n_3$) represents the ratio of the change in the differential phase between TM- and TE-polarization ($\Delta\phi$) to the change in the refractive index of the binding layer (sensing medium) (Δn_3). And the second term, E is the adsorption efficiency of the target biomolecule on the binding layer. We assume that

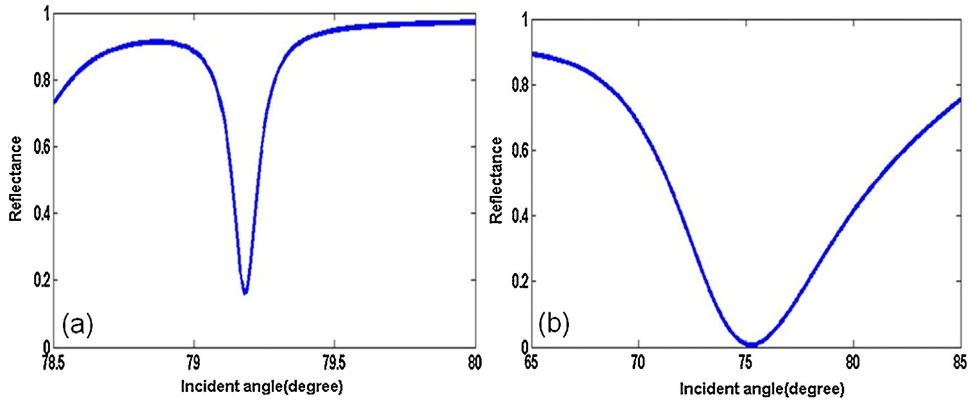

Fig. 2. Simulated reflectance diagram using TM polarization: (a) for proposed biosensor configuration, observed resonance angle is 79.2° and (b) for surface plasmon resonance biosensor, observed resonance angle is 75.25°.

the refractive index of binding layer (n_3) increases from 1.462 to 1.466 in an interval of 0.0001, when the adsorption of biomolecules occurs and hence the total refractive index change is given by, $\Delta n_3 = 0.004$. The relative differential phase change between TM- and TE-polarization with refractive index of sensing medium is shown in Fig. 3. Fig. 3(a) and (b), respectively represent the differential phase change curve of proposed biosensor and surface plasmon resonance biosensor, and both curves linearly increase when the refractive index of the sensing medium increases. In the case of proposed configuration, relative differential phase change varies from 135° to 183° for the total refractive index change of 0.004, while the surface plasmon resonance biosensor has a slight variation of 99.7° to 103° for the same refractive index change. Hence the calculated sensitivity for proposed biosensor and surface plasmon resonance biosensor are 1.2×10^4 °/RIU and 8.25×10^2 °/RIU, respectively. It shows that the sensitivity of the proposed configuration is 14.8 times more than those of a surface plasmon resonance biosensor.

The influence of number of graphene layers in the 1D PC on sensitivity enhancement is also investigated and plotted in Fig. 4(a). It is found that the maximum sensitivity is observed when the 1D PC consists of single layer graphene and there is a sudden decrease in sensitivity for bilayer graphene. After that the sensitivity is almost constant when the graphene layers in the PC increases. It can be attributed presumably to the reduction in light intensity due to the increase of graphene layers (2.3% light absorption in the case of monolayer graphene). It shows that the proposed configuration can provide maximum sensitivity when the photonic crystal consists of single layer graphene. The sensitivity variation of the surface plasmon resonance biosensor is also analyzed by varying the thickness of the gold thin film (as shown in Fig. 4(b)). In this case, the Au film thickness is varied from 30 nm to 60 nm and maximum sensitivity is observed for 45 nm. This thickness (45 nm) represents the optimum thickness for maximum sensitivity and the corresponding sensitivity value is almost equal to those of a 4 layer graphene-based proposed sensor. In addition, the sensitivity of biosensor configuration has been studied by varying the number of bilayers (graphene/PMMA) and note that maximum sensitivity is obtained for 9 bilayers. Further, we observed that the sensitivity of the proposed configuration decreases when the excitation wavelengths increases. It could be due to the increase of graphene extinction coefficient with increase in excitation wavelengths.

In order to confirm the existence of surface electromagnetic waves in the proposed biosensor configuration, the surface electromagnetic field distribution is simulated using finite difference time domain (FDTD) method. In the simulation, the graphene thickness is assumed as 1 nm and hence the smallest spatial grid size of 0.1 nm is used for the iteration to maintain the accuracy and stability of FDTD calculations. Here we assume that the light is incident at a resonant coupling angle of 79.2° through the prism. The electric field distribution and its magnitude as a function of depth along the 1D PC is shown in Fig. 5. Note that the output electric field is normalized with respect to the incident excitation field. It is visible from the figure that the intensity is decaying toward the prism/1D PC interface and field oscillates many times throughout the periodic structure. It is also clear from the figure that when the surface mode is excited, the electromagnetic field enhancement occurs within the last layer of the 1D PC (1D PC/binding layer interface). It shows that the mode at the band edge has less attenuation and thus the decaying evanescent filed can penetrate much

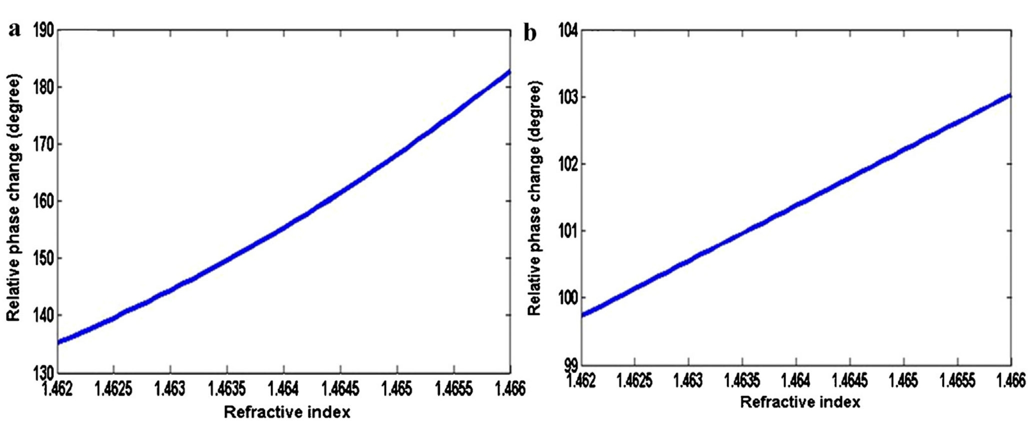

Fig. 3. Variation of relative phase change with refractive index of binding layer (a) for proposed configuration and (b) for surface plasmon resonance biosensor.

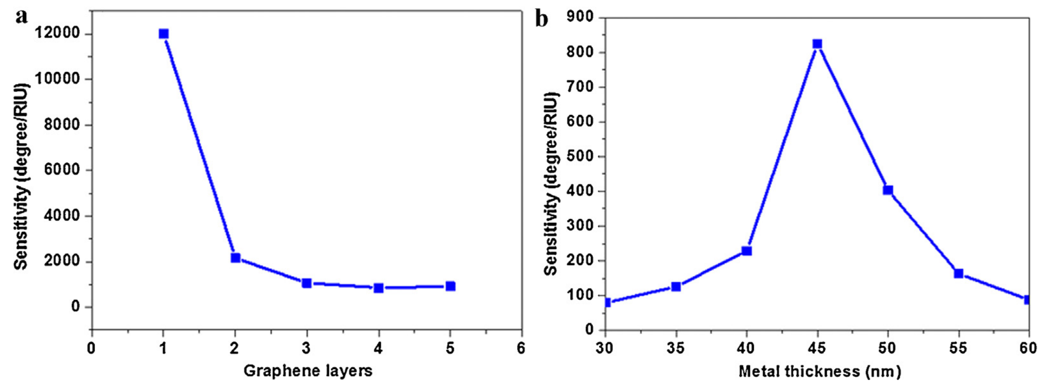

Fig. 4. Sensitivity variation as a function of (a) number of graphene layers (for proposed configuration) and (b) gold thin film thickness (for surface plasmon resonance biosensor).

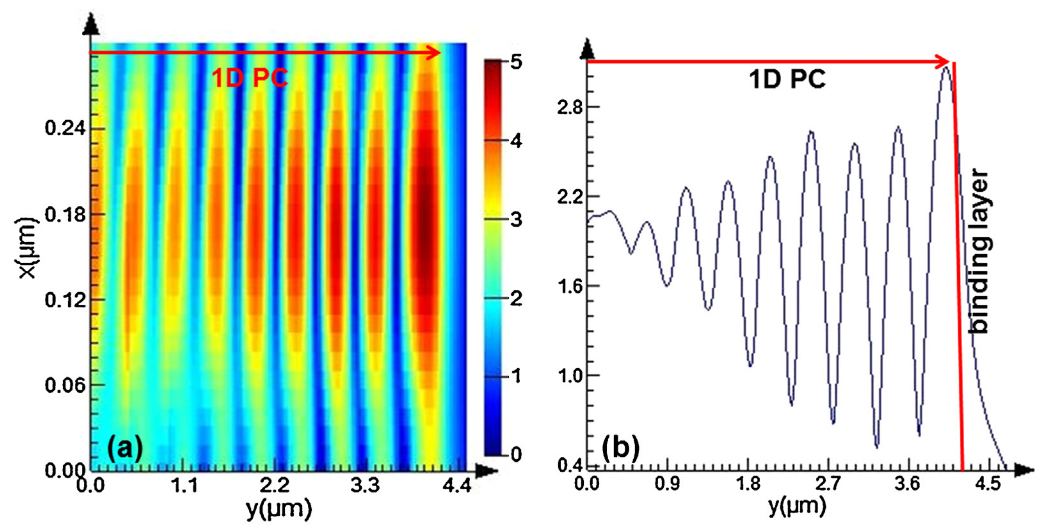

Fig. 5. Simulated electromagnetic field distributions along the *y*-direction of the proposed graphene-based photonic crystal biosensor, (a) electric field distribution in 2D plane and (b) its magnitude as a function of depth along the multilayer.

further into 1D PC. Maximum field enhancement factor is observed at PC/binding layer interface, which is due to the tighter confinement of mode to the surface. This large enhancement factor is responsible for the observed enhanced sensitivity of the proposed graphene-based 1D PC biosensor. In addition, the excitation of SEW in the proposed structure can be confirmed by studying the surface dispersion diagram [13]. As reported in our previous work [13], the SEW exists in the non-radiative region of the surface dispersion diagram and away from the air light line. It means that SEWs cannot radiate either into the air side or into the 1D PC. The parallel wave vector of the mode calculated at 633 nm incident wavelength using the expression $(2\pi/\lambda)n_0 \sin\theta$ is 1.476×10^7 rad/m. We found that this value occur close to the second band edge and appear away from the air light line, which further confirm the excitation of SEW in the proposed graphene-based biosensor configuration.

4. Conclusion

A biosensor configuration based on the excitation of surface electromagnetic waves in a graphene-based 1D photonic crystal is presented and the results are then compared with those of a conventional surface plasmon resonance biosensor. The existence of SEW in the proposed biosensor configuration is numerically investigated for enhanced sensitivity. About 15% increment in sensitivity is obtained compared to surface plasmon resonance biosensor and it is also evident from the results that the number of graphene layer is an important parameter to be considered for improving the sensitivity when designing efficient biosensor geometries. The experimental study is needed to further support the proposed concept.

Acknowledgments

The authors acknowledge the financial support received through National Research Foundation NRF RF Award No. NRF-RF2010-07.

References

[1] J. Homola, Present and future of surface plasmon resonance biosensors, Analytical and Bioanalytical Chemistry 377 (2003) 528–539.
[2] Z. Shuwen, Y. Ken-Tye, R. Indrajit, D. Xuan-Quyen, Y. Xia, L. Feng, A review on functionalized gold nanoparticles for biosensing applications, Plasmonics 6 (2011) 491–506.
[3] K.V. Sreekanth, R. Sidharthan, V.M. Murukeshan, Gap modes assisted enhanced broadband light absorption in plasmonic thin film solar cell, Journal of Applied Physics 110 (2011) 033107.
[4] K. Sathiyamoorthy, R. Sidharthan, K.V. Sreekanth, V.M. Murukeshan, Dye assisted enhanced transmission in near field optical lithography, Optics Communication 283 (2010) 5245–5249.
[5] J.B. Khurgin, A. Boltasseve, Reflecting upon the lossesin plasmonics and metamaterials, MRS Bulletin 37 (2012) 768–779.
[6] K. Sathiyamoorthy, K.V. Sreekanth, R. Sidharthan, V.M. Murukeshan, B. Xing, Surface plasmon enhancement in gold nanoparticles in the presence of an optical gain medium: an analysis, Journal of Physics D: Applied Physics 44 (2011) 425102.

[7] F. Villa, L.E. Regalado, F. Ramos-Mendieta, J. Gaspar-Armenta, T. Lopez-Ríos, Photonic crystal sensor based on surface waves for thin-film characterization, Optics Letters 27 (2002) 646–648.
[8] K. Kim, E.-J. Cho, Y.-M. Huh, D. Kim, Thin-film-based sensitivity enhancement for total internal reflection fluorescence live-cell imaging, Optics Letters 32 (2007) 3062–3064.
[9] Y. Wan, Z. Zheng, W. Kong, X. Zhao, Y. Liu, Y. Bian, J. Liu, Nearly three orders of magnitude enhancement of Goos–Hanchen shift by exciting Bloch surface wave, Optics Express 20 (2012) 8998–9003.
[10] M. Shinn, W.M. Robertson, Surface plasmon-like sensor based on surface electromagnetic waves in a photonic band-gap material, Sensors and Actuators B 105 (2005) 360–364.
[11] W.M. Robertson, Experimental measurement of the effect of termination on surface electromagnetic waves in one-dimensional photonic bandgap arrays, Journal of Lightwave Technology 17 (1999) 2013–2017.
[12] W.M. Robertson, M.S. May, Surface electromagnetic wave excitation on one-dimensional photonic band-gap arrays, Applied Physics Letters 74 (1999) 1800.
[13] K.V. Sreekanth, S. Zeng, J. Shang, K. Yong, T. Yu, Excitation of surface electromagnetic waves in a graphene-based Bragg grating, Scientific Reports 2 (737) (2012), http://dx.doi.org/10.1038/srep00737.
[14] C. Cong, T. Yu, R. Saito, G.F. Dresselhaus, M.S. Dresselhaus, Second-order overtone and combination Raman modes of graphene layers in the range of 1690–2150 cm(−1), ACS Nano 5 (2011) 1600–1605.
[15] F. Bonaccorso, Z. Sun, T. Hasan, A.C. Ferrari, Graphene photonics and optoelectronics, Nature Photonics 4 (2010) 611–622.
[16] J. Shang, T. Yu, J. Lin, G.G. Gurzadyan, Ultrafast electron-optical phonon scattering and quasiparticle lifetime in CVD-grown graphene, ACS Nano 5 (2011) 3278–3283.
[17] M. Jablan, H. Buljan, M. Soljacic, Plasmonics in graphene at infrared frequencies, Physical Review B 80 (2009) 245435.
[18] R.R. Nair, P. Blake, A.N. Grigorenko, K.S. Novoselov, T.J. Booth, T. Stauber, N.M.R. Peres, A.K. Geim, Fine structure constant defines visual transparency of graphene, Science 320 (2008) 1308-1308.
[19] O.L. Berman, R.Y. Kezerashvili, Graphene-based one-dimensional photonic crystal, Journal of Physics: Condensed Matter 24 (2012) 015305.
[20] H. Benisty, Graphene nanoribbons: photonic crystal waveguide analogy and minigap stripes, Physical Review B 79 (2009) 155409.
[21] H. Yan, X. Li, B. Chandra, G. Tulevski, Y. Wu, M. Freitag, W. Zhu, P. Avouris, F. Xia, Tunable infrared plasmonic devices using graphene/insulator stacks, Nature Nanotechnology 7 (2012) 330–334.
[22] L. Wu, H.S. Chu, W.S. Koh, E.P. Li, Highly sensitive graphene biosensors based on surface plasmon resonance, Optics Express 18 (2010) 14395–14400.
[23] S.H. Choi, Y.L. Kim, K.M. Byun, Graphene-on-silver substrates for sensitive surface plasmon resonance imaging biosensors, Optics Express 19 (2011) 446–458.
[24] R. Verma, B.D. Gupta, R. Jha, Sensitivity enhancement of a surface plasmon resonance based biomolecules sensor using graphene and silicon layers, Sensors and Actuators B 160 (2011) 623–631.
[25] P.K. Maharana, R. Jha, Chalcogenide prism and graphene multilayer based surface plasmon resonance affinity biosensor for high performance, Sensors and Actuators B 169 (2012) 161–166.
[26] M. Bruna, S. Borini, Optical constants of graphene layers in the visible range, Applied Physics Letters 94 (2009) 031901.
[27] F. Ramos-Mendieta, P. Halevi, Propagation constant-limited surface modes in dielectric superlattices, Optics Communication 129 (1996) 1–5.
[28] E.D. Palik, Handbook of Optical Constant of Solids, Academic Press, Inc., Orlando, 1985.
[29] .S.Y. Wu, H.P. Ho, W.C. Law, C. Lin, S.K. Kong, Highly sensitive differential phase-sensitive surface plasmon resonance biosensor based on the Mach-Zehnder configuration, Optics Letters 29 (2004) 2378–2380.
[30] S. Zeng, X. Yu, W.C. Law, Y. Zhang, R. Hu, X.Q. Dinh, H.P. Ho, K.T. Yong, Size dependence of Au NP-enhanced surface plasmon resonance based on differential phase measurement, Sensors and Actuators B 176 (2013) 1128–1133.
[31] S.H. Choi, K.M. Byun, Investigation on an application of silver substrates for sensitive surface plasmon resonance imaging detection, Journal of the Optical Society of America A: Optics and Image Science 10 (2010) 2229–2236.

Biographies

Kandammathe Valiyaveedu Sreekanth received his Ph.D degree from School of Mechanical and Aerospace Engineering, Nanyang Technological University, Singapore. He is currently working as a Postdoctoral Fellow at School of Physics and Mathematical Sciences, Nanyang Technological University, Singapore. His main research interests include nanofabrication, plasmonics, and graphene.

Shuwen Zeng is currently a Ph.D student of the School of Electrical and Electronic Engineering at Nanyang Technological University. Her research interests mainly focus on enhanced surface plasmon resonance biosensors based on graphene and gold nanoparticles (Au NPs).

Ken-Tye Yong received his Ph.D from Chemical and Biological Engineering in SUNY at Buffalo in 2006. Following completion of his graduate studies, he did his post-doc at the Institute for Lasers, Photonics and Biophotonics from 2006 to 2009. He is currently an Assistant Professor at the Nanyang Technological University in the School of Electrical and Electronic Engineering. His research interests include nanostructured materials for sensing applications and quantum dots for cancer therapy.

Ting Yu is a Nanyang Assistant Professor in the Division of Physics and Applied Physics, School of Physical and Mathematical Sciences at Nanyang Technological University, a joint assistant professor of Department of Physics, Faculty of Science, National University of Singapore and a National Research Foundation fellow. He obtained his Ph.D degree from National University of Singapore (NUS) and completed a post-doctoral study in NUS under the Singapore Millennium Foundation (SMF) Postdoctoral Fellowship. His research interests include Raman spectroscopy and nanocarbons, carbon-metal oxide nanohybrids for nanoelectronics, nanophotonics and sustainable energy.